

Metal complexes of hexaazatriphenylene (hat) and its derivatives— from oligonuclear complexes to coordination polymers

Susumu Kitagawa*, Shigeyuki Masaoka

*Department of Synthetic Chemistry and Biological Chemistry, Graduate School of Engineering,
Kyoto University, Katsura, Nishigyo-ku, Kyoto 615-8510, Japan*

Contents

Abstract	73
1. Introduction	74
2. Synthesis of hat and its derivatives	75
3. Structural classification of metal complexes	75
3.1. Lower nuclearity compounds: mono-, bi-, and trinuclear complexes	75
3.2. Nanometer-sized oligomeric compounds	76
3.2.1. Multi-decker compounds	76
3.2.2. Cyclic compounds	76
3.2.3. Dendritic compounds	77
3.3. Assembled networks of low molecular weight modules	77
3.3.1. Hydrogen bond-linked networks	77
3.3.2. π - π Stack-linked networks	78
3.4. Infinite coordination polymers	79
3.4.1. One-dimensional chain structures	79
3.4.2. Two-dimensional layer structures	80
3.4.3. Three-dimensional structures	80
4. Properties	81
4.1. Anion-trapping	81
4.2. Photophysical properties	84
4.3. Nonlinear optics	86
4.4. Magnetic properties	86
5. Conclusion	87
Acknowledgements	87
References	87

Abstract

Metal complexes of hexaazatriphenylene (hat) and its derivatives are reviewed, focusing on assembled structures based on their X-ray crystallographic structures. A wide variety of crystal structures of mononuclear, binuclear, trinuclear and oligonuclear complexes and coordination polymers are classified by the coordination modes such as bidentate, bis-bidentate, and tris-bidentate forms of the ligands, their synthetic procedures being developed from serendipitous to rational level. Their magnetic, electrochemical, photophysical properties, and molecular inclusions are described. The ligand, hat, discussed here is one of the most useful multifunctional ligands, affording not only various self-assembled frameworks but also unique electronic structures. Their characteristics are mentioned in detail.

© 2003 Elsevier B.V. All rights reserved.

Keywords: Hexaazatriphenylene; π -Electronic system; Multidentate ligand; Electron acceptor; Coordination polymer; Supramolecular assembly; Metal-to-ligand charge transfer; Magnetic properties; Nonlinear optics

* Corresponding author. Tel.: +81-75-753-5652; fax: +81-75-753-7979.

E-mail address: kitagawa@schem.kyoto-u.ac.jp (S. Kitagawa).

1. Introduction

A large number of metal complexes have been extensively synthesized in this half century, focusing on mono- or binuclear metal complexes. On the other hand, oligo- and polynuclear complexes are expected to provide a variety of physical and chemical properties such as magnetism, electric conductivity, molecular adsorption, heterogeneous catalysis, and/or ion exchange. Of particular interest are oligo- and polynuclear complexes containing multifunctional ligands with π -electronic structures which provide unique electronic properties.

Hexaazatriphenylene (hat) and its derivatives have been studied as attractive supramolecular building blocks, because of their characteristic features as follows. First, the ligands have three chelating sites to the metal ions, which are useful for the construction of the metal-assembled system. Second, the ligands afford characteristic electron-deficient π -systems, which exhibit metal-to-ligand charge transfer and/or readily undergo reduction to form paramagnetic radical ligands. Third, the ligands have a C_3 symmetry axis, leading to degenerate π^* orbitals and octupole moment in essence. Finally, the ligands afford a variety of interesting chemical/physical properties based on their electronic structures which can readily be modified by their six substituent groups.

Oligo- and polynuclear complexes with hat and its derivatives afford intriguing crystal structures depending on the coordination modes of hat, i.e. single, double, and triple metal-chelating (Figs. 1–3, respectively), and range from discrete complexes to infinite coordination polymers. Although discrete complexes or one-dimensional coordi-

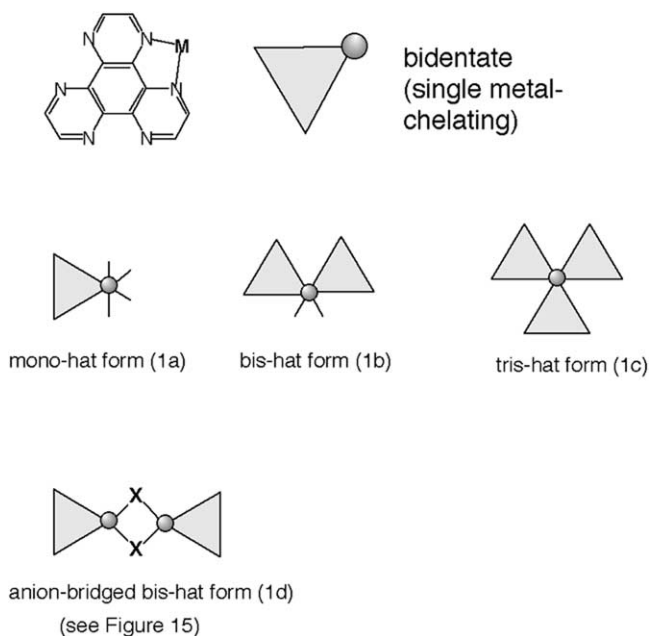


Fig. 1. Schematic structures of bidentate (single metal-chelating) complexes of hat derivatives.

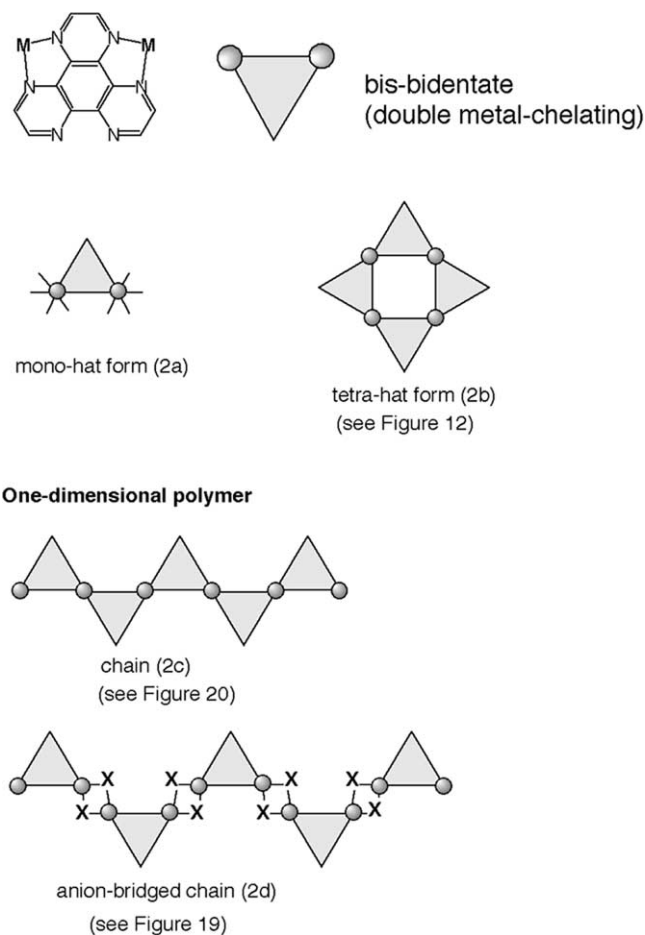


Fig. 2. Schematic structures of bis-bidentate (double metal-chelating) complexes of hat derivatives.

dination polymers cover most of the oligo- and polynuclear complexes, hydrogen bonding and π – π stacking can also cause supramolecular assembly to construct higher-dimensional structures. Consequently, the solid state structures are classified into four types: lower nuclearity compounds, nanometer-sized oligomeric compounds, infinite supramolecular assemblies of low molecular weight modules, and infinite coordination polymers. Crystallographically characterized compounds containing both finite and infinite molecular assemblies are listed in Table 3. Because of the characteristic multifunctionalities of hat and its derivatives, their metal complexes afford intriguing crystal structures and physicochemical properties. In practice, electrochemical, magnetic and/or photophysical properties have added a new dimension to coordination chemistry, and this family is opening up a field of hat-based materials, akin to that of the porphyrins.

This article begins with a description of the synthesis of hat and its derivatives. In the following paragraphs, we survey their structural coordination chemistry, focusing on supramolecular assemblies and coordination polymers, and then, discuss the physicochemical properties of metal

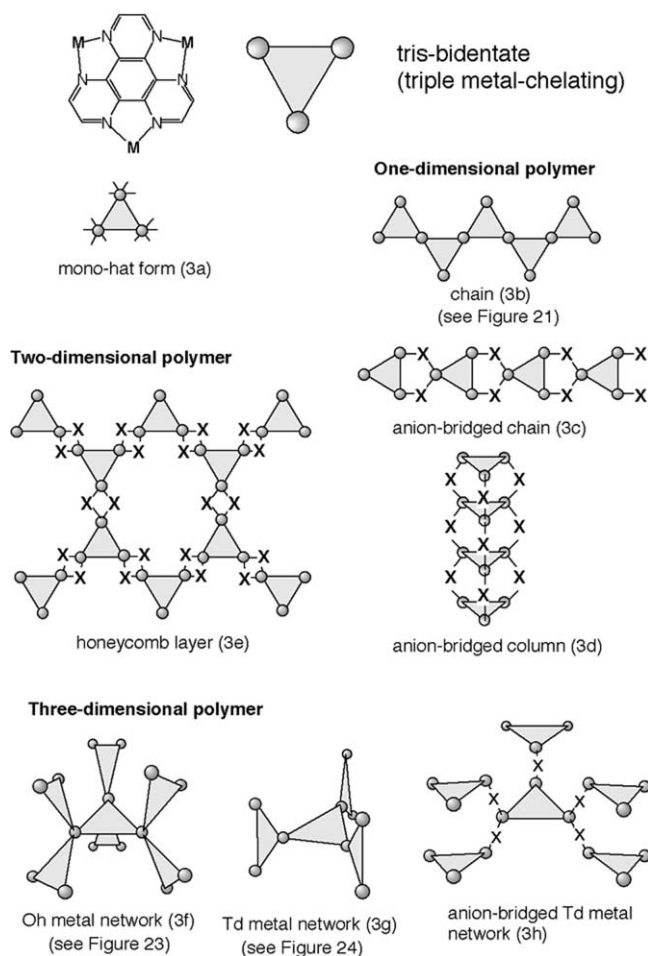


Fig. 3. Schematic structures of tris-bidentate (triple metal-chelating) complexes of hat derivatives.

complexes with hat derivatives, in relation not only to basic chemistry but also to material chemistry.

2. Synthesis of hat and its derivatives

Two main synthetic approaches to hat and its derivatives have been reported: one is the reaction of hexaaminobenzene with 1,2-diketone [1–3], and the other is between hexaketocyclohexane (triquinoyl) and 1,2-diaminoethylene derivatives (Fig. 4) [4–7]. The former route affords a variety of hat derivatives, e.g. alkyl-, aryl-, and vinyl-derivatives. However, this route needs many steps to final products and employs triaminotrinitrobenzene, which is used as an explosive in military applications. On the other hand, the latter method is relevant to synthesize hat derivatives with electron-withdrawing groups, e.g. cyano-, carboxyl-, and amide-derivatives. They show characteristic low coordination ability of the aromatic nitrogen atoms due to the six electron-withdrawing groups. These hat derivatives are summarized in Table 1 (Table 2).

3. Structural classification of metal complexes

3.1. Lower nuclearity compounds: mono-, bi-, and trinuclear complexes

A variety of the mononuclear (1a type), binuclear (2a type) and trinuclear (3a type) complexes with a single hat molecule are listed in Table 3 (crystallographically characterized compounds) and Table 4 (crystallographically uncharacterized compounds, which was generally characterized by $^1\text{H-NMR}$ and mass spectrometry). Among these complexes, mononuclear and binuclear complexes are considered as candidates for a synthon of supramolecular assemblies because of the further coordination ability of the remaining metal-free chelate sites.

A series of Ru, Rh and Ir complexes with parent hat ligand (Table 4), e.g. $[\text{Ru}(\text{bpy})_2(\text{hat})]^{2+}$, $[\{\text{Ru}(\text{bpy})_2\}_2(\text{hat})]^{4+}$, $[\text{Rh}(\text{ppy})_2(\text{hat})]^+$, and $[\text{Ir}(\text{ppy})_2(\text{hat})]^+$ (bpy=2,2'-bipyridine, ppy=2-phenylpyridine), is obtained by the reaction of hat with the corresponding building blocks such as $[\text{Ru}(\text{bpy})_2]^{2+}$, $[\text{Rh}(\text{ppy})_2]^+$, and $[\text{Ir}(\text{ppy})_2]^+$, respectively [8–16]. These complexes are characterised by the combination of NMR, FAB- and ESI-MS, and HPLC. Moreover, the stepwise reaction can afford the heterometal complexes, e.g. $[\{\text{Ru}(\text{bpy})_2\}\{\text{Rh}(\text{ppy})_2\}(\text{hat})]^{3+}$, and $[\{\text{Ru}(\text{bpy})_2\}\{\text{Ir}(\text{ppy})_2\}(\text{hat})]^{3+}$ [10]. The HPLC data of these polymetallic compounds reveal that the trimetallic homo- and heteronuclear complexes (3a type) are not stable under chromatographic conditions in some organic solvents.

Hexaazatriphenylene hexacarbonitrile hat-(CN)₆ acts as a unique multidentate ligand because its electron-deficient heterocyclic core has low-lying degenerate π^* orbitals. Preparation of metal complexes containing the hat-(CN)₆ ligand is extremely difficult because the coordination ability of the aromatic nitrogen atoms in hat-(CN)₆ drastically decreases due to the presence of the six electron-withdrawing cyano groups. The one-electron reduction of hat-(CN)₆ efficiently enhances its coordinating ability, and we have been able to isolate transition metal complexes, $[\{\text{Cu}(\text{dppe})\}_3\{\text{hat}(\text{CN})_6\}](\text{CF}_3\text{SO}_3)_2$ (3a type) and $[\{\text{Cu}(\text{dppe})\}_3\{\text{hat}(\text{CN})_6\}](\text{PF}_6)_2$ (3a type), which contain stable radical anions, $[\text{hat}(\text{CN})_6]^-$. Interestingly, the product was obtained in a one-pot reaction of a copper(I) source, hat-(CN)₆, and dppe in acetone (Fig. 5) [17]. The thin-layer cyclic voltammogram of $[\{\text{Cu}(\text{dppe})\}_3\{\text{hat}(\text{CN})_6\}](\text{PF}_6)_2$ in THF shows multiredox couples at $E_{1/2}=+0.47$, $+0.18$, -0.16 , and -0.91 V (vs. SCE), which are assigned to $[\text{hat}(\text{CN})_6](0/-\text{I})$, $[\text{hat}(\text{CN})_6](-\text{I}/-\text{II})$, $[\text{hat}(\text{CN})_6](-\text{II}/-\text{III})$, and $[\text{hat}(\text{CN})_6](-\text{III}/-\text{IV})$, respectively. Thus, the ligand hat-(CN)₆ is in the one-electron reduced state at the rest potential ($+0.27$ V). Interestingly, all the waves in $[\{\text{Cu}(\text{dppe})\}_3\{\text{hat}(\text{CN})_6\}](\text{PF}_6)_2$ undergo remarkable positive shifts compared with those in metal-free hat-(CN)₆ ($E_{1/2}=-0.05$ (0/-I), -0.43 (-I/-II), and -1.01 (-II/-III) V (vs. SCE)), indicating that the acceptor capability of the

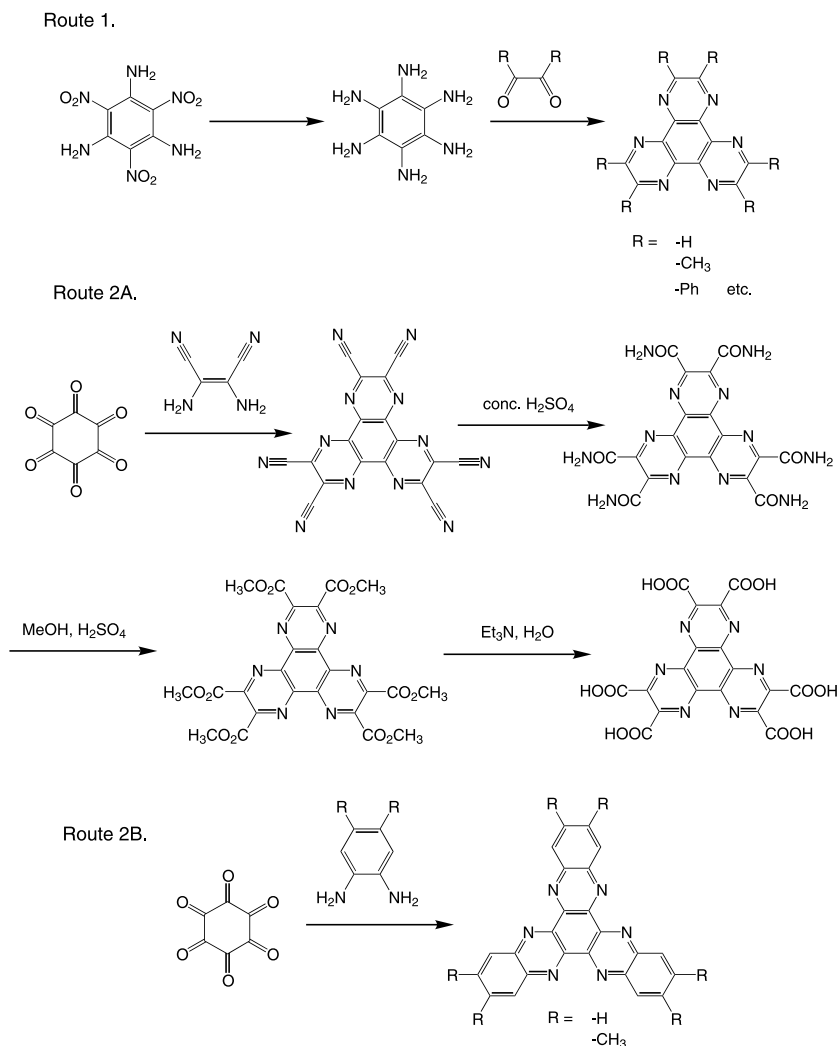


Fig. 4. Syntheses of hat and its derivatives.

hat-(CN)₆ moiety is enhanced by coordination of the three copper(I) atoms.

3.2. Nanometer-sized oligomeric compounds

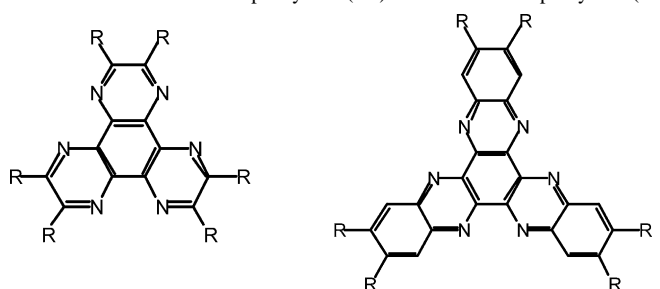
3.2.1. Multi-decker compounds

One of the most famous complexes which contains a hat derivative is a so-called ‘double-decker’ compound (analogue of 3d type) resulting from the spontaneous assembly process of 11 components (Fig. 6) [18–20]. Moreover, hat-Ph₆ ligands and a series of linear polypyridyl ligands set up the framework with the aid of copper(I) or silver(I) ions to generate the large cage-like entities (Figs. 7 and 8) [21]. The processes amount to the spontaneous assembly of a total of 15 and 19 components to yield multicompartamental architectures. The crystal structures of such complexes have been determined. They confirm the nature of the entities formed and show that, in addition, several substrate species (anions and solvent molecules) are contained in the cavities.

3.2.2. Cyclic compounds

Molecular self-assembly with cyclic topology is one of the most useful methods to design and construct nanometer-sized polynuclear metal complexes [22,23]. Recently, reported was the novel cyclic hexamer containing a hat derivative, whose coordination topology is controlled by the carboxylate groups and classified in a different category from Figs. 1–3. The deprotonated form of hat-(COOH)₆, [hat-(COO)₆]⁶⁻, functions as a right angle linker, which is useful for constructing a cyclic nanostructure (Fig. 9) [24]. A cyclic hexamer with chair-like connectivity forms when cobalt(II) nitrate solutions in MeCN are layered onto basic aqueous solutions of ligand. Fig. 10 represents a cyclic framework, which preferentially forms according to the design shown in Fig. 9. The cyclic module (Fig. 11) has an S₆-symmetrical screw-like structure. For cyclic nanostructures, it is very important to control not only the angle of the subunit linker but also the template guest. In this case, a hexaaquacobalt(II) cation ([Co(H₂O)₆]²⁺) is encapsulated in the central cavity of the cyclic hexamer (Fig. 11). The

Table 1
Abbreviations of hexaazatriphenylene (hat) and hexaazatrinaphthylene (htn)



The image shows the chemical structures of the hexaazatriphenylene (hat) and hexaazatrinaphthylene (htn) ligands. The hat ligand is a central benzene ring fused with six pyridine rings at the 1, 2, 3, 4, 5, and 6 positions. The htn ligand is a central benzene ring fused with six naphthalene rings at the 1, 2, 3, 4, 5, and 6 positions. Both ligands have six R groups at the outer positions of the fused rings.

R	Abbreviation	Synthetic route	References
hat derivatives			
H	hat	1 and 2A	[1–3,7–16,25,27,28,30,32–34,40,41,43,44]
Ph	hat-Ph ₆	1	[3,18–21]
CN	hat-(CN) ₆	2A	[4,5,17,29,46]
COOH	hat-(COOH) ₆	2A	[4,5,7,24,29]
CONH ₂	hat-(CONH ₂) ₆	2A	[4,5,29]
CH=CH-Ar	hat-(CH=CH-Ar) ₆	1	[47]
htn derivatives			
H	htn	2B	[34]
Me	hhtn	2B	[36]

water molecules of the guest complex are hydrogen-bonded to carboxylate groups from the cyclic hexamer, contributing well to the stability of the cyclic framework.

Molecular square [Co₄(hat)₄Cl₈] (2b type) is also synthesized from the addition of aqueous solutions of hat and CoCl₂ in a 1:1 ratio (Fig. 12) [25]. Slow evaporation of the water led to the formation of orange prismatic crystals of the product.

3.2.3. Dendritic compounds

Dendrimers have also been developed [26] as nanometer-sized molecules constructed by rational synthetic strategy. A dendric heptanuclear complex of Ru(II), [Ru(hat)₃{Ru(phen)₂}₆]¹⁴⁺ (analogue of 3f type), was synthesized and characterized by electrospray mass spectrometry

(ESI-MS) [27]. The synthetic method is as follow. First, 1c-type [Ru(hat)₃]Cl₂ is prepared from Ru(dmsO)₄Cl₂ and three hat ligands. This central core contains six new chelating sites to which six units can be grafted to yield the heptametallic complex (Fig. 13). Ru(phen)₂Cl₂ pretreated with AgNO₃, reacts with [Ru(hat)₃]²⁺ (6:1 ratio) during 48 h, to give rise to [Ru(hat)₃{Ru(phen)₂}₆]¹⁴⁺, isolated by precipitation with ammonium hexafluorophosphate. The heptametallic complex [Ru(hat)₃{Ru(phen)₂}₆](PF₆)₁₄ in dichloromethane or acetonitrile was directly analyzed by ESI-MS.

Moreover, the STM imaging of the heptanuclear Ru(II) dendrimer has been successfully observed [28]. STM imaging was carried out on a mono-add layer of the Ru(II) dendrimer formed by physisorption from a 1,2,4-trichlorobenzene solution at the liquid–graphite interface. The packing of the molecules on the surface was visualized by the formation of ordered patterns and a distance of 27 Å was measured between two adjacent lamellae.

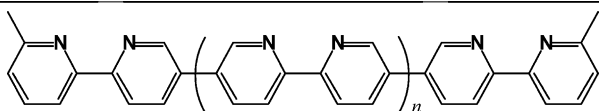
3.3. Assembled networks of low molecular weight modules

3.3.1. Hydrogen bond-linked networks

Electron-withdrawing groups (e.g. –CN, –CO₂R, CONR₂) on the hat afford π-systems much more electron-deficient than the parent hat. This electron deficiency influences their assembled structures in the solid state, having propensity for weakly π–π stacked assemblies. Indeed, the X-ray structures of hat-(COOH)₆ and hat-(COOMe)₆ reveal rigorous avoidance of hat–hat π-stacking. However, the structure of hexamide hat-(CONH₂)₆ reveals intra- and intermolecular hydrogen bonding with concomitant π–π stacking [29]. The hat-(CONH₂)₆ molecules stack

Table 2
Abbreviations of other ligands mentioned in this review

Abbreviation	Ligand	References
sq ^{2–}	Squarate dianion	[30]
ox ^{2–}	Oxalate dianion	[30]
dppe	Bis(1,2-diphenylphosphino)ethane	[17,46]
bpy	2,2′-Bipyridine	[8–11,13–16,40]
phen	1,10-Phenanthroline	[11,12,15,41,43,44]
ppy	2-Phenylpyridine	[10,13]
Me ₂ bpy	5,5′-Dimethylbipyridine	[47]
tetrapy	See below (n=0)	[18–21]
spy	See below (n=1)	[21]
octapy	See below (n=2)	[21]



The structures of tetrapy (n=0), spy (n=1), and octapy (n=2).

Table 3
Crystallographically characterized compounds

Compound	Coordination mode	Type	Figures	References
Discrete compounds				
[Cu(hat)(H ₂ O) ₃ (sq)]·3H ₂ O	bidentate	1a	–	[30]
[Cu(hat)(H ₂ O)(ox)]·H ₂ O	bidentate	1d	Figs. 15–17	[30]
[Cu(hat) ₂ (H ₂ O) ₂](ClO ₄) ₂ ·4H ₂ O	bidentate	1b	–	[30]
[{Cu(dppe)} ₃ {hat-(CN) ₆ }] (CF ₃ SO ₃) ₂	tris-bidentate	3a	Figs. 5 and 26	[17,46]
[{Cu(dppe)} ₃ {hat-(CN) ₆ }] (PF ₆) ₂	tris-bidentate	3a	Figs. 5 and 27	[17,46]
[Re(CO) ₃ Cl(hhtn)]	bidentate	1a	–	[31]
[{PdCl ₂ }{Re(CO) ₃ Cl}(hhtn)]	bis-bidentate	2a	–	[31]
[PdCl ₂ (hhtn)]	bidentate	1a	Fig. 18	[31]
Nanometer-sized oligomeric compounds				
[Co ₆ {hat-(COO) ₆ }] ²⁴⁻	tri- and quadridentate	–	Figs. 9–11	[24]
[Co ₄ (hat) ₄ Cl ₈]	bis-bidentate	2b	Fig. 12	[25]
[Cu ₆ (tetrapy) ₃ {hat-(Ph) ₆ }] ⁶⁺	tris-bidentate	analogue of 3d	Fig. 6	[18–21]
[Cu ₉ (spy) ₃ {hat-(Ph) ₆ }] ⁹⁺	tris-bidentate	analogue of 3d	Fig. 7	[21]
[Cu ₁₂ (octapy) ₃ {hat-(Ph) ₆ }] ¹²⁺	tris-bidentate	analogue of 3d	Fig. 8	[21]
Coordination polymers				
[Cu ₄ (hat) ₂ Cl ₈]·6H ₂ O] _n	bis-bidentate, 1D	2d	Fig. 19	[32]
[Cu(hat)(H ₂ O) ₂](NO ₃) ₂] _n	bis-bidentate, 1D	2c	Fig. 20	[32]
[Cu ₂ (hat)(H ₂ O) ₆](SO ₄) ₂ ·2H ₂ O] _n	tris-bidentate, 1D	3b	Fig. 21	[32]
[Co ₃ (hat){N(CN) ₂ }] ₆ (H ₂ O) ₂] _n	tris-bidentate, 1D	3c	–	[33]
[Co(H ₂ O) ₆] ₁₀ [Co ₆ {Co(H ₂ O) ₃ }] ₂ {hat-(COO) ₆ }] _n	mono-, tri-, and quadridentate, 2D	–	Fig. 22	[24]
[Ag(hat)](ClO ₄) _n	tris-bidentate, 3D	3f	Fig. 23	[34]
[Ag ₃ (hnt) ₂](NO ₃) ₃] _n	tris-bidentate, 3D	3g	Figs. 24 and 25	[36]

in a closely packed arrangement, although spacing of the molecules in the stack is not uniform. Closely spaced dimers are observed with a one-half ring offset that permits HOMO–LUMO overlap (Fig. 14). The mean interplanar distance of the HAT rings within these dimers, 3.32(10) Å, is smaller than the sum of van der Waals radii and consistent with π -complexation.

The hydrogen bond-linked assembly of discrete complexes is observed in the crystal structure of [Cu(hat)(H₂O)(ox)]·H₂O (ox²⁻=oxalate dianion) [30]. The neutral mononuclear building blocks [Cu(hat)(H₂O)(ox)] feature single metal-chelating hat, oxalate coordinating in the equatorial plane of copper and water molecule binding in axial position (Fig. 15). Pairs of such units are joined into 1d-type binuclear entities through semi-coordination to a neighboring oxalate. The molecules are arranged side-by-side into a sheet structure. Within the sheets weak O(ox)···H(hat)

and N(hat)···H(hat) interactions stabilize the arrangement (Fig. 16). Between sheets the solvent water molecules form links to the neighboring sheet through hydrogen bonding (Fig. 17). These hat molecules partially overlap at an interplanar distance of 3.25 Å, indicating the presence of π – π interaction.

3.3.2. π – π Stack-linked networks

The crystal structure of [PdCl₂(hhtn)] (1a type) shows the one dimensional assembly through π – π stacking [31]. The reaction of hhtn with 1 equiv of Pd(NCPH)₂Cl₂ gave orange crystals, whose asymmetric unit has two independent but strongly interacting [PdCl₂(hhtn)] molecules. This intimate association is shown in Fig. 18. The structure consists of a nearly square planar PdCl₂(N₂) complex in a highly distorted hhtn framework. An unfavorable Cl···H interaction forces the PdCl₂ unit out of the hhtn plane by 28.1°. The

Table 4
Crystallographically uncharacterized compounds, which were generally characterized by ¹H-NMR and mass spectrometry

Compound	Coordination mode	Type	References
[{Cu(Me ₂ bpy)} ₃ {hat-(C=CAr) ₆ }] (PF ₆) ₂	tris-bidentate	3a	[47]
[Ru(hat) ₃ {Ru(phen) ₂ }] ₆] ¹⁴⁺	tris-bidentate	analogue of 3f	[27,28]
[{Ru(bpy) ₂ }{Re(CO) ₃ Cl} ₂ (hat)] ²⁺	tris-bidentate	3a	[14]
[{Ru(bpy) ₂ }] _n (hat)] ²ⁿ⁺ (n=1–3)	mono-, bis-, and tris-bidentate	1a, 2a, and 3a	[8–11,13–16,40]
[{Ru(phen) ₂ }] _n (hat)] ²ⁿ⁺ (n=1–3)	mono-, bis-, and tris-bidentate	1a, 2a, and 3a	[11,12,15,41,43,44]
[Ru(bpy) _{3–n} (hat) _n] ²⁺ (n=1–3)	bidentate	1a, 1b, and 1c	[9,11,13]
[{Ru(bpy) ₂ }] ₂ {Os(bpy) ₂ }(hat)] ⁶⁺	tris-bidentate	3a	[16]
[M(ppy) ₂ (hat)] ⁺ (M=Rh, Ir)	bidentate	1a	[10,13]
[{Rh(ppy) ₂ }] ₂ (hat)] ²⁺	bis-bidentate	2a	[10]
[{Ru(bpy) ₂ }{Rh(ppy) ₂ }(hat)] ³⁺	bis-bidentate	2a	[10]
[{Ru(bpy) ₂ }{Ir(ppy) ₂ }(hat)] ³⁺	bis-bidentate	2a	[10]

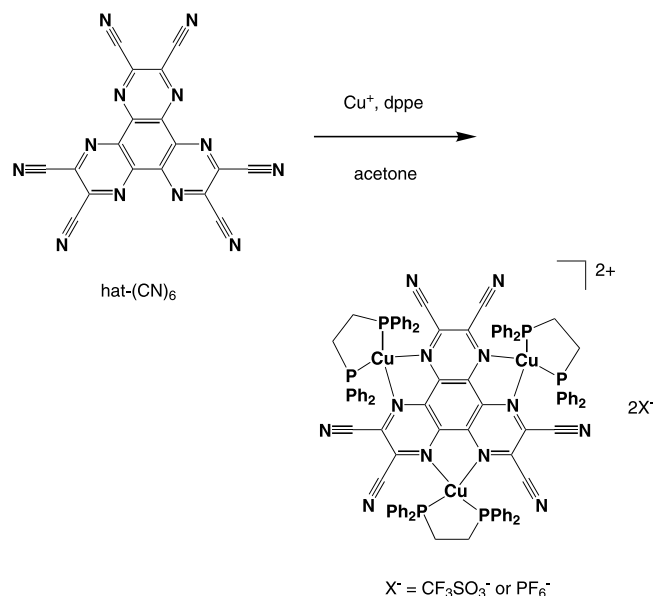


Fig. 5. Synthesis of $[\{\text{Cu}(\text{dppe})\}_3\{\text{hat-(CN)}_6\}]^{2+}$. The complex contains stable radical anion, $[\text{hat-(CN)}_6]^-$, coordinating to three copper(I) ions.

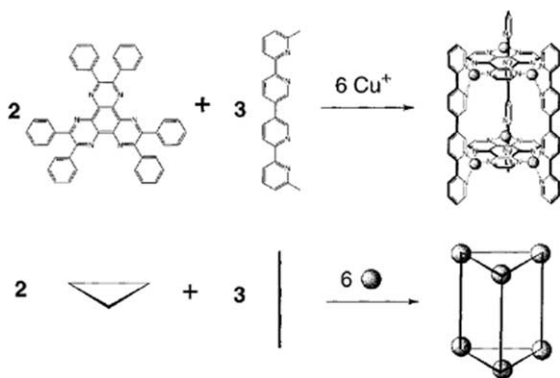


Fig. 6. Spontaneous assembly of $[\text{Cu}_6(\text{tetrapy})_3\{\text{hat-(Ph)}_6\}_2]^{6+}$. The structure is schematically represented as an analogue of 3d type in Fig. 3 (original Figure 1 from Ref. [20]).

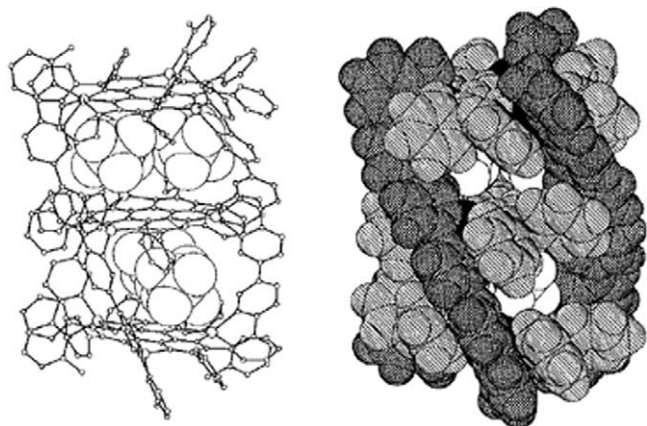


Fig. 7. Crystal structure of $[\text{Cu}_9(\text{spy})_3\{\text{hat-(Ph)}_6\}_3]^{9+}$. The structure is schematically represented as an analogue of 3d type in Fig. 3 (original Figure 4 from Ref. [21]).

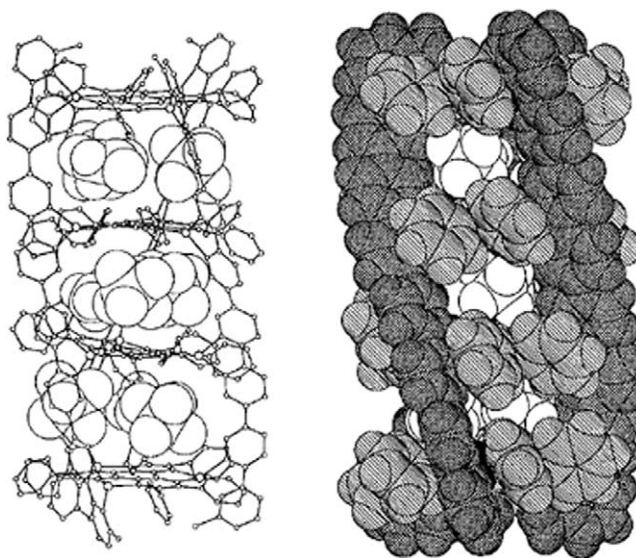


Fig. 8. Crystal structure of $[\text{Cu}_{12}(\text{octapy})_3\{\text{hat-(Ph)}_6\}_4]^{12+}$. The structure is schematically represented as an analogue of 3d type in Fig. 3 (original Figure 5 from Ref. [21]).

structure indicates that there are π – π (hat–hat) interactions, forming a one-dimensional column. The complexes adopt a staggered configuration, with the PdCl_2 portions directed approximately 180° apart from each other. The molecules adopt an alternating convex–concave, concave–convex relationship.

3.4. Infinite coordination polymers

3.4.1. One-dimensional chain structures

There are four types of infinite one-dimensional chains. Three of them, $\{[\text{Cu}_4(\text{hat})_2\text{Cl}_8] \cdot 6\text{H}_2\text{O}\}_n$ (2d type), $\{[\text{Cu}(\text{hat})(\text{H}_2\text{O})_2](\text{NO}_3)_2\}_n$ (2c type), and $\{[\text{Cu}_2(\text{hat})(\text{H}_2\text{O})_6](\text{SO}_4)_2 \cdot 2\text{H}_2\text{O}\}_n$ (3b type), are obtained by the reactions of parent hat with copper(II) ions [32]. The basic building block in $\{[\text{Cu}_4(\text{hat})_2\text{Cl}_8] \cdot 6\text{H}_2\text{O}\}_n$ is the binuclear $[\text{Cu}_2(\text{hat})\text{Cl}_4]$ entity, two such units being connected to tetranuclear units through relatively strong axial Cu–Cl bonds (Fig. 19). In $\{[\text{Cu}(\text{hat})(\text{H}_2\text{O})_2](\text{NO}_3)_2\}_n$ and $\{[\text{Cu}_2(\text{hat})(\text{H}_2\text{O})_6](\text{SO}_4)_2 \cdot 2\text{H}_2\text{O}\}_n$ hat-bridged copper(II) chains are present (Figs. 20 and 21). The hat serves as a bis- and tris-bidentate ligand in $\{[\text{Cu}(\text{hat})(\text{H}_2\text{O})_2](\text{NO}_3)_2\}_n$ and $\{[\text{Cu}_2(\text{hat})(\text{H}_2\text{O})_6](\text{SO}_4)_2 \cdot 2\text{H}_2\text{O}\}_n$, respectively; in the latter compound one of the copper atoms coordinated to hat does not participate in the chain formation. The copper geometries observed in these compounds are square pyramidal and elongated octahedral.

The aqueous reaction of CoSO_4 , $\text{Na}[\text{N}(\text{CN})_2]$, and hat affords the dicyanamide-linked coordination polymer $\{[\text{Co}_3(\text{hat})\{\text{N}(\text{CN})_2\}_6(\text{H}_2\text{O})_2]\}_n$ (3c type) [33]. Unfortunately, the crystal structure is not completely solved and the composition, $\{[\text{Co}_3(\text{hat})\{\text{N}(\text{CN})_2\}_6(\text{H}_2\text{O})_2]\}_n$, was decided based on elemental analysis.

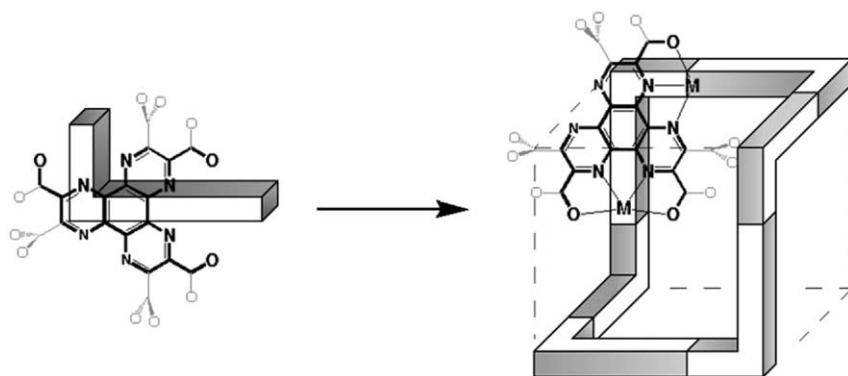


Fig. 9. Schematic representation of design and self-assembly of a cyclic nanostructure. The ligand $[\text{hat}(\text{COO})_6]^{6-}$ acts as a building block with a right angle (original Figure 1b from Ref. [24]).

3.4.2. Two-dimensional layer structures

A two-dimensional structure is obtained by linking the hexagonal cyclic modules, $[\text{Co}_6\{\text{hat}(\text{COO})_6\}_6]^{24-}$ (Fig. 11) [24]. The residual carboxylate groups, which do not join the cyclic formation, act as the secondary interaction site to link the cyclic units. The coordination of the carboxylate groups to another cobalt(II) cations provides a facial-type coordination geometry with the six oxygen atoms from the three water molecules and the three carboxylate groups forming a two-dimensional honeycomb layer on the *ab* plane (Fig. 22).

3.4.3. Three-dimensional structures

Two types of three-dimensional networks involving hat derivatives are obtained by coordination with silver(I) ions. One is obtained as orange crystals of $\{[\text{Ag}(\text{hat})]\text{ClO}_4 \cdot 2\text{CH}_3\text{NO}_2\}_n$ (3f type) with a chiral space

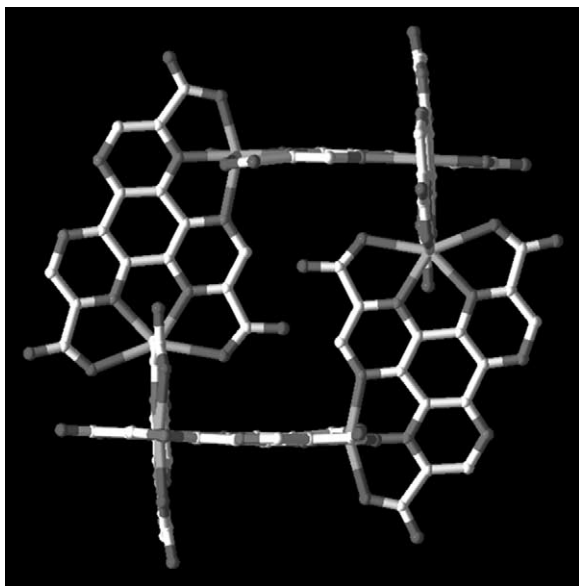


Fig. 10. Crystal structure of $[\text{Co}_6\{\text{hat}(\text{COO})_6\}_6]^{24-}$. Carboxylate groups which do not join in the formation of the cycle are omitted for clarity (original Figure 3 from Ref. [24]).

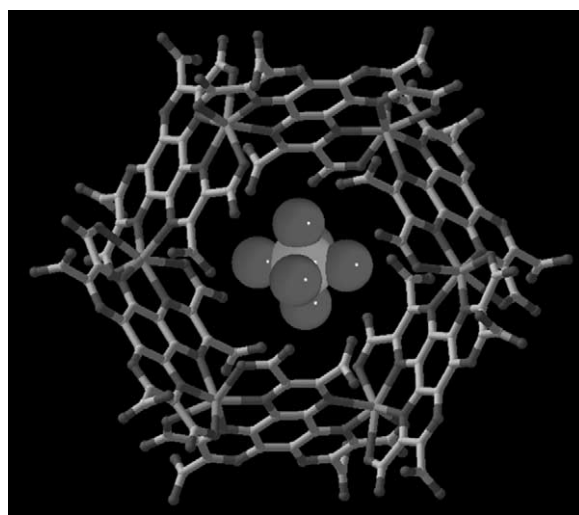


Fig. 11. Crystal structure of $[\text{Co}_6\{\text{hat}(\text{COO})_6\}_6]^{24-}$ along *c* axis. A hexaaquacobalt(II) cation is encapsulated in the cavity of the cyclic module, hydrogen-bonded to carboxylate groups from the cyclic hexamer (original Figure 4 from Ref. [24]).

group by diffusing hat in nitromethane with AgClO_4 in acetonitrile [34]. All the silver centers are equivalent, being chelated by three hat ligands which provide an N_6 coordination environment intermediate between octahedral and trigonal prismatic. The ligands are also all equivalent, each chelating three metal centers (Fig. 23). The nitromethane molecules are located in the micropores as crystal solvents. Each nitromethane molecule associates with two neighbors,

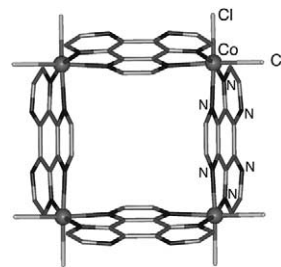


Fig. 12. Crystal structure of $[\text{Co}_4(\text{hat})_4\text{Cl}_8]$. The structure is schematically represented as 2b type in Fig. 2.

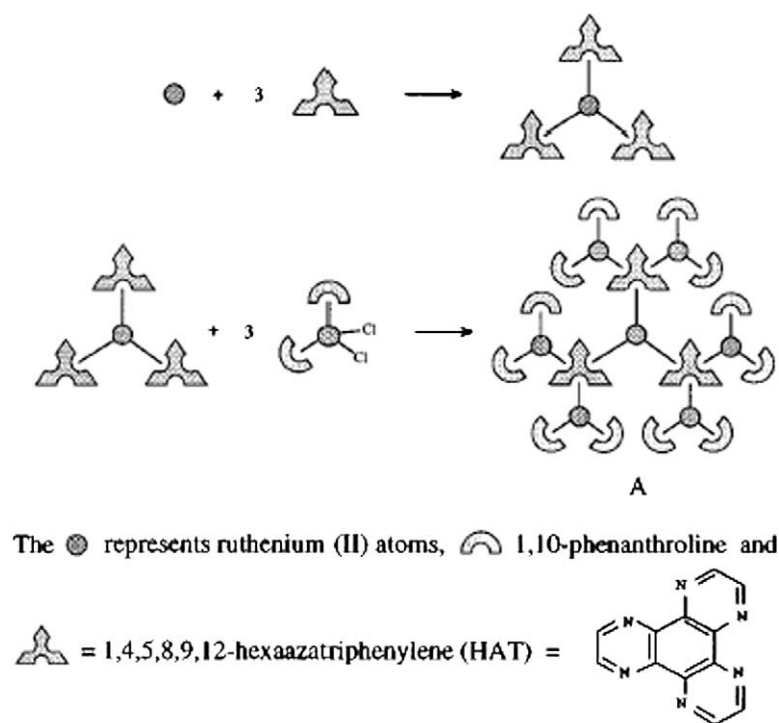


Fig. 13. Schematic representation of synthesis of $[\text{Ru}(\text{hat})_3\{\text{Ru}(\text{phen})_2\}_6]^{14+}$. The structure is schematically represented as analogue of 3f type in Fig. 3 (original Scheme 1 from Ref. [27]).

making very close $\text{N}^{\delta+} \cdots \text{O}^{\delta-}$ contacts (3.02 Å), similar to the contact observed in the crystal structure of nitromethane itself (3.00–3.07 Å) [35].

The other network $\{[\text{Ag}_3(\text{htn})_2](\text{NO}_3)_3\}_n$ (3g type) is prepared by layering a solution of AgNO_3 in acetonitrile

on top of a solution of htn in dichloromethane [36]. In the case of $\{[\text{Ag}_3(\text{htn})_2](\text{NO}_3)_3\}_n$ each Ag(I) center acts as a two-connecting node by linking two htn ligands. Interestingly, the htn exhibits twofold interpenetrating networks with the two-connected Ag(I) nodes and three-connected htn (Fig. 24). These two three-dimensional networks are topologically equivalent but have different threefold helices (Fig. 25), where the two arrows show the handedness of helices. Thus, $\{[\text{Ag}_3(\text{htn})_2](\text{NO}_3)_3\}_n$ contains an interpenetrating enantiomorphic pair.

4. Properties

4.1. Anion-trapping

Molecule-trapping by synthetic receptors is one of the most attractive areas in the field of host–guest chemistry, and the complexation of anions has recently been recognised and developed as a new area of coordination chemistry [37]. We reported the anion trapping behaviour of the complex $[\{\text{Cu}(\text{dppe})\}_3\{\text{hat}(\text{CN})_6\}]^{2+}$, which is well-illustrated for $[\{\text{Cu}(\text{dppe})\}_3\{\text{hat}(\text{CN})_6\}](\text{CF}_3\text{SO}_3)_2$ in Fig. 26 [17]. Six phenyl groups of the three dppe ligands create concave cavities on each side of the planar $[\text{hat}(\text{CN})_6]^-$ unit, into which the CF_3SO_3^- ions are effectively trapped. The inclusion occurs on both sides of the cation. Compound $[\{\text{Cu}(\text{dppe})\}_3\{\text{hat}(\text{CN})_6\}](\text{PF}_6)_2$ has essentially the same anion trapping structure in the solid state.

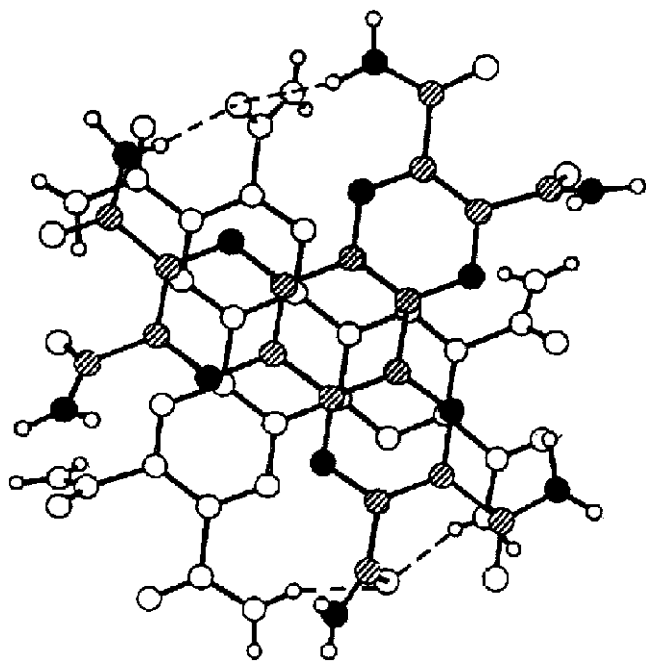


Fig. 14. Hydrogen bonding of $\text{hat}(\text{CONH}_2)_6$ (original Figure 1 from Ref. [29]).

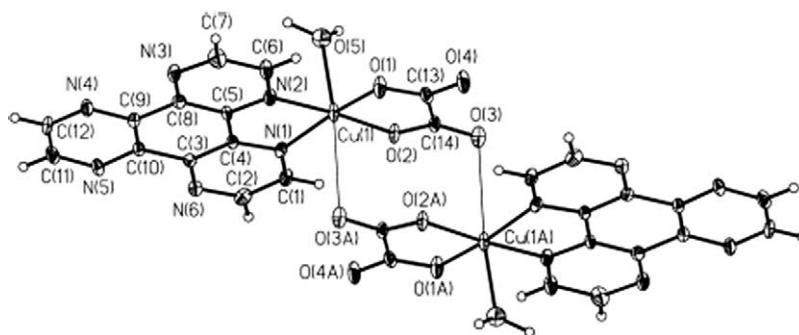


Fig. 15. Crystal structure of dimeric $[\text{Cu}_2(\text{hat})_2(\text{H}_2\text{O})_2(\text{ox})_2]$. The structure is schematically represented as 1d type in Fig. 1 (original Figure 1 from Ref. [30]).

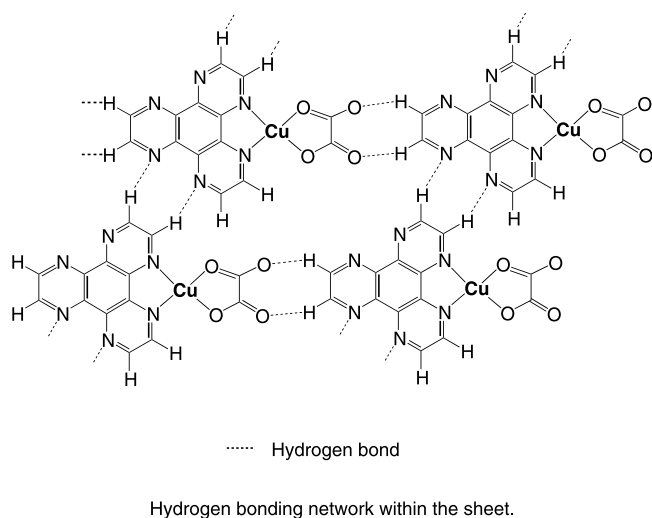


Fig. 16. Hydrogen bond-linked network within the sheet.

The anion radical ligand $[\text{hat}(\text{CN})_6]^\bullet$ in $[\{\text{Cu}(\text{dppe})\}_3\{\text{hat}(\text{CN})_6\}](\text{PF}_6)_2$ facilitates the evaluation of the host–guest interaction in solution by conventional NMR techniques. The ^{31}P -NMR resonance for the PF_6^- ion of $n\text{Bu}_4\text{NPF}_6$ and $[\{\text{Cu}(\text{dppe})\}_3\{\text{hat}(\text{CN})_6\}](\text{PF}_6)_2$ in CDCl_3 at room temperature is given in Fig. 27a and b, respectively. Fig. 27b shows an extremely broad signal at $\delta = -134.1$ (septet $J(^{19}\text{F}, ^{31}\text{P}) = 713 \pm 10$ Hz), which is shifted downfield relative to that for the free PF_6^- ion (Fig. 27a). Due to the absence of a direct bonding interaction between the radical center and the counterion PF_6^- , the temperature-dependence of the chemical shift is simply accounted for by the paramagnetic effect (pseudo-contact term; $\delta_{\text{pseudo-com}}$). By using the slope of a linear plot of the observed chemical shift for PF_6^- against T^{-1} , the separation between the $\text{hat}(\text{CN})_6$ center and the observed nucleus was estimated to be 3.3 Å. The separation is quite similar to the distance (3.9 Å) estimated from

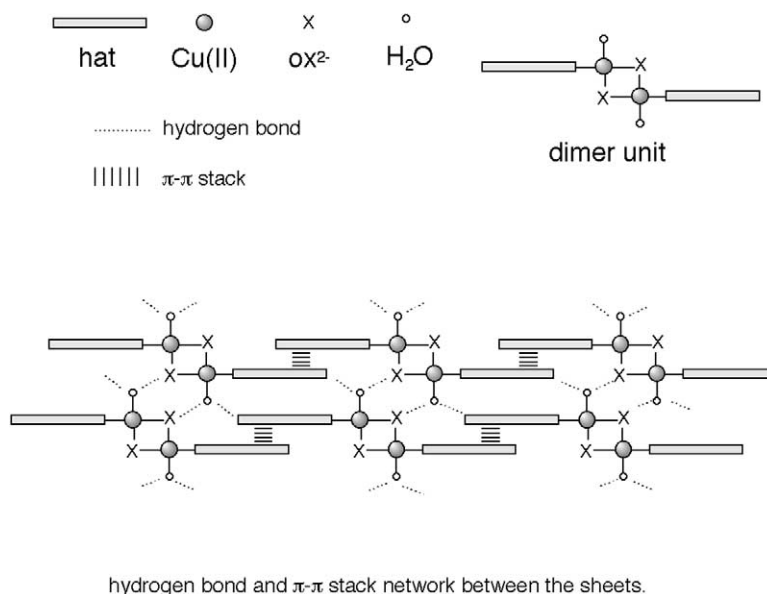


Fig. 17. Hydrogen bond and π - π stack-linked network between the sheets.

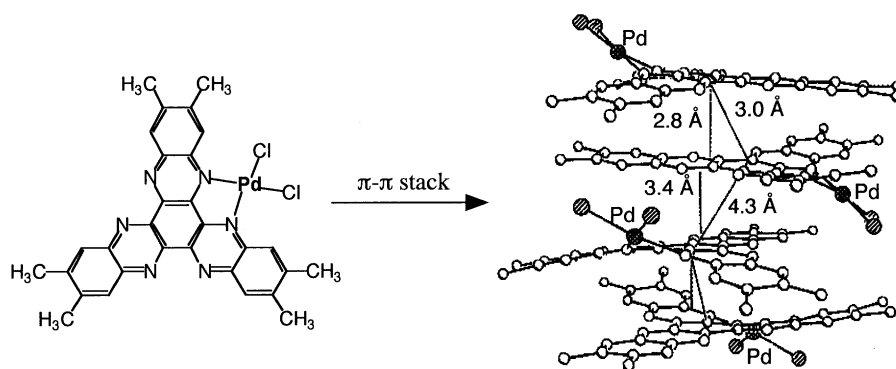


Fig. 18. π - π Stack-linked network of $[\text{PdCl}_2(\text{hhtn})]$ (original Figure 3 from Ref. [31]).

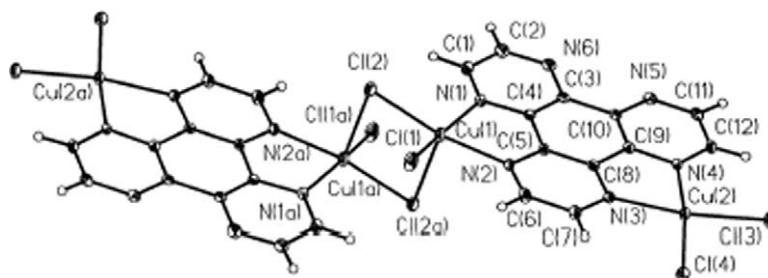


Fig. 19. Crystal Structure of $\{[\text{Cu}_4(\text{hat})_2\text{Cl}_8] \cdot 6\text{H}_2\text{O}\}_n$. The structure is schematically represented as 2d type in Fig. 2 (original Figure 1 from Ref. [32]).

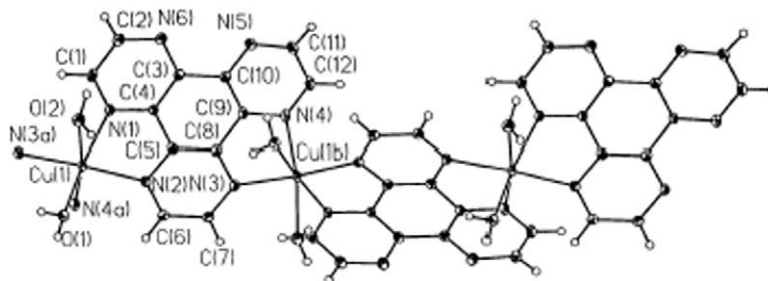


Fig. 20. Crystal structure of $\{[\text{Cu}(\text{hat})(\text{H}_2\text{O})_2](\text{NO}_3)_2\}_n$. The structure is schematically represented as 2c type in Fig. 2 (original Figure 3 from Ref. [32]).

the crystal structure analysis, which clearly indicates that the anion sits in a position so close to the hat-(CN)₆ ligand and that the electronic-nuclear spin magnetic interaction operates effectively. Thus, the PF_6^- ion is well-trapped

in the positively charged concave cavities, even in solution.

The addition of sodium *p*-toluenesulfonate ($\text{CH}_3\text{C}_6\text{H}_4\text{SO}_3\text{Na}$) to a CDCl_3 solution of $\{[\text{Cu}(\text{dppe})_3\{\text{hat}-(\text{CN})_6\}]\}$

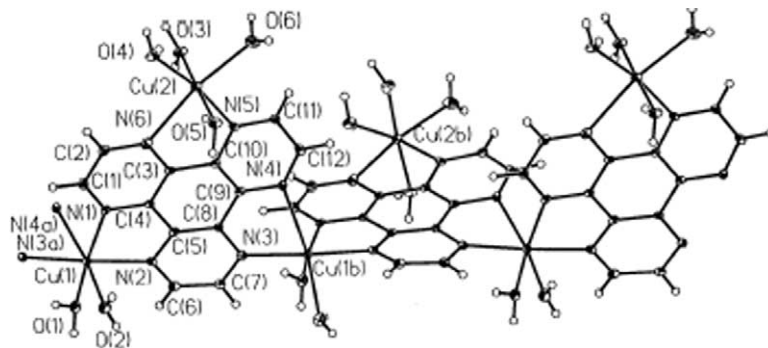


Fig. 21. Crystal structure of $\{[\text{Cu}_2(\text{hat})(\text{H}_2\text{O})_6](\text{SO}_4)_2 \cdot 2\text{H}_2\text{O}\}_n$. The structure is schematically represented as 3b type in Fig. 3 (original Figure 4 from Ref. [32]).

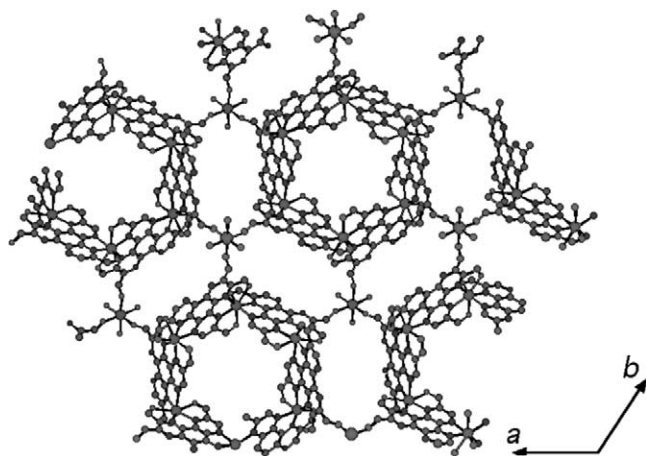


Fig. 22. Honeycomb layer structure of $[\text{Co}_6\{\text{hat}-(\text{COO})_6\}_6]^{24-}$ in the ab plane (original Figure 5 from Ref. [24]).

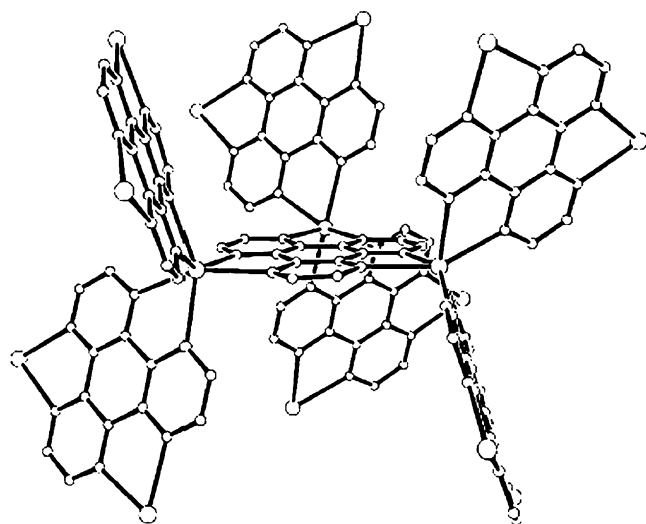


Fig. 23. Crystal structure of $\{[\text{Ag}(\text{hat})](\text{ClO}_4)\}_n$. The structure is schematically represented as 3f type in Fig. 3 (original Figure 1 from Ref. [34]).

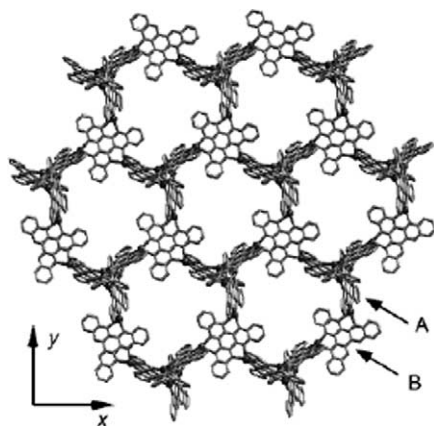


Fig. 24. Crystal structure of $\{[\text{Ag}_3(\text{htn})_2](\text{NO}_3)_3\}_n$. The structure is schematically represented as 3g type in Fig. 3 (original Figure 1a from Ref. [36]).

$(\text{PF}_6)_2$, resulted in an upfield shift of the ^{31}P -NMR resonance for the PF_6^- ion (Fig. 28). After the addition of 2 equiv of sodium *p*-toluenesulfonate, the chemical shift became identical to that of $n\text{Bu}_4\text{NPF}_6$, indicating that two positively charged concave cavities of $[\{\text{Cu}(\text{dppe})_3\}\{\text{hat}-(\text{CN})_6\}]^{2+}$ prefer the inclusion of $\text{CH}_3\text{C}_6\text{H}_4\text{SO}_3^-$ to that of PF_6^- .

The anion trapping behaviour is also observed in the multi-decker complexes [21]. As revealed by the crystal structures shown in Fig. 7, anions are contained in the cavities. Their presence is also reflected in the ^1H -NMR signals of $[\text{Cu}_9(\text{spy})_3\{\text{hat}-(\text{Ph})_6\}_3](\text{PF}_6)_9$ and $[\text{Cu}_9(\text{spy})_3\{\text{hat}-(\text{Ph})_6\}_3](\text{CF}_3\text{SO}_3)_9$. When 9 equiv of $n\text{Bu}_4\text{NCF}_3\text{SO}_3$ were added to $[\text{Cu}_9(\text{spy})_3\{\text{hat}-(\text{Ph})_6\}_3](\text{PF}_6)_9$, the chemical shifts became identical to those of $[\text{Cu}_9(\text{spy})_3\{\text{hat}-(\text{Ph})_6\}_3](\text{CF}_3\text{SO}_3)_9$ after 24 h. On the other hand, when 9 equiv of $n\text{Bu}_4\text{NPF}_6$ were added to $[\text{Cu}_9(\text{spy})_3\{\text{hat}-(\text{Ph})_6\}_3](\text{CF}_3\text{SO}_3)_9$, the chemical shifts remained unchanged on standing for 24 h in CD_3NO_2 . The anions are therefore able to move into and out of the cavities at room temperature but cationic moiety $[\text{Cu}_9(\text{spy})_3\{\text{hat}-(\text{Ph})_6\}_3]^{9+}$ appears to have a distinct preference for the inclusion of CF_3SO_3^- in the presence of PF_6^- .

4.2. Photophysical properties

$\text{Ru}(\text{II})$ -polypyridine complexes have been the subject of many investigations resulting in a fairly good understanding of their electrochemical and photophysical properties [38,39]. In recent years the research in this area has been extended from the study of monometallic compounds to the development of polymetallic supramolecular systems, which may have considerable potential as the basis of materials designed for use in photochemical molecular devices. The poly ruthenium complexes containing hat and its derivatives, which are regarded as C_3 symmetric polypyridine ligands with low-lying π electronic system, are expected to afford interesting electrochemical and photophysical properties based on the metal-to-ligand charge transfer and/or electron-deficient π systems. In this section, three interesting topics about $\text{Ru}(\text{II})$ -hat complexes are introduced.

In binuclear and trinuclear $\text{Ru}(\text{II})$ -hat complexes $[\{\text{Ru}(\text{bpy})_2\}_2(\text{hat})]^{4+}$ (2a type) and $[\{\text{Ru}(\text{bpy})_2\}_3(\text{hat})]^{6+}$ (3a type), the individual centers are tris-bidentate in nature, affording right- or left-handed chirality (designated Δ or Λ respectively) [15,40,41]. The stereoisomers (meso ($\Delta\Delta$) and rac ($\Delta\Delta/\Lambda\Lambda$)) of the diruthenium(II) complexes $[\{\text{Ru}(\text{bpy})_2\}_2(\text{hat})]^{4+}$ have been isolated by a combination of synthetic methods and chromatographic techniques involving mononuclear precursors of predetermined chirality. Additionally, the homochiral (Δ^3/Λ^3) and heterochiral ($\Delta^2\Lambda/\Lambda^2\Delta$) diastereomers of the triruthenium(II) complexes $[\{\text{Ru}(\text{bpy})_2\}_3(\text{hat})]^{6+}$, and the enantiomers of both forms, have been isolated and identified. Emission studies of all the binuclear species at room temperature indicate that the relative luminescence quantum yields and emission lifetimes significantly decrease for the meso compound

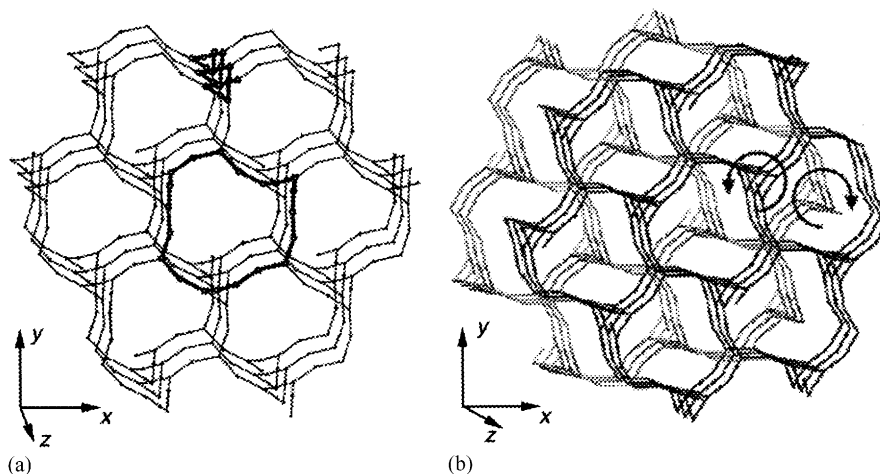


Fig. 25. Schematic view of $\{[\text{Ag}_3(\text{htn})_2](\text{NO}_3)_3\}_n$ in which the ligands are replaced by trigonal nodes (original Figure 2c from Ref. [36]).

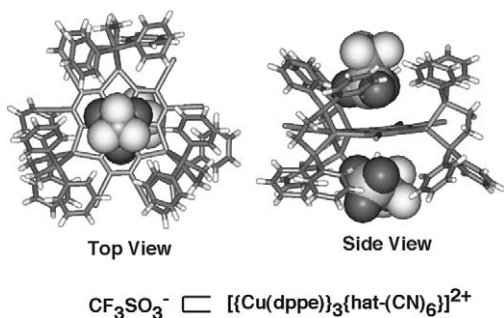


Fig. 26. Anion trap structure of $[\{\text{Cu}(\text{dppe})\}_3\{\text{hat}(\text{CN})_6\}](\text{CF}_3\text{SO}_3)_2$.

with the rac diastereomers. In the case of trinuclear complexes, no significant differences were detected at room temperature in the diastereoisomers. However, in a glass at low temperature (80 K), the luminescence lifetimes of the trinuclear heterochiral diastereomer were slightly shorter than those of the hemochiral form.

For the series of dimetallic homo- and heteronuclear complexes containing Ru, Rh and Ir, $[\{\text{Ru}(\text{bpy})_2\}_2(\text{hat})]^{4+}$,

$[\{\text{Ru}(\text{bpy})_2\}\{\text{Rh}(\text{ppy})_2\}(\text{hat})]^{3+}$, $[\{\text{Ru}(\text{bpy})_2\}\{\text{Ir}(\text{ppy})_2\}(\text{hat})]^{3+}$, electrochemical and photophysical properties are reported [10]. Upon electrochemical reduction of these complexes, the first reduction wave involves hat-centered π^* orbitals. Therefore, on the basis of the electrochemical, luminescence and resonance Raman data, the lowest electronic transitions are CT (charge transfer) transitions involving the bridging hat. These transitions have an MLCT (metal-to-ligand charge transfer) type for the Ru(II) moiety and a SBLCT (σ -bond to ligand charge transfer) character for the Rh(III) unit. In the case of $[\{\text{Ru}(\text{bpy})_2\}\{\text{Ir}(\text{ppy})_2\}(\text{hat})]^{3+}$, an important energy transfer process is observed. The electrochemical data indicate that closely lying Ir–C σ -bonding and Ir $d\pi$ orbitals are located above the Ru-centered $d\pi$ level. This suggests the presence of Ir–hat SBLCT mixed with Ir–hat MLCT absorption bands. On the basis of these considerations the luminescence from $[\{\text{Ru}(\text{bpy})_2\}\{\text{Ir}(\text{ppy})_2\}(\text{hat})]^{3+}$ should be regarded as a result of a strong admixture of Ir–hat $^3\text{SBLCT}$ and $^3\text{MLCT}$ character, also characteristic of the monometallic $[\{\text{Ir}(\text{ppy})_2\}(\text{hat})]^+$ complex. The excitation

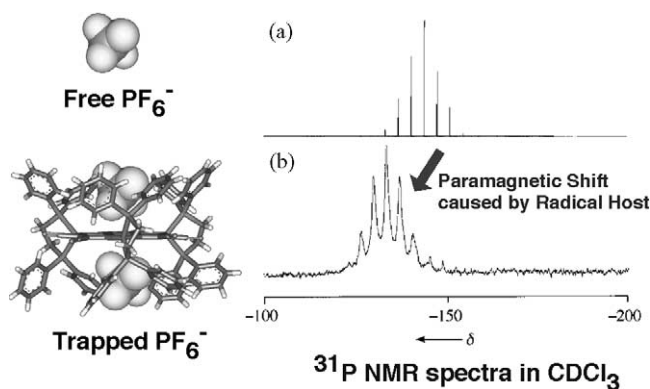


Fig. 27. ^{31}P -NMR spectra at room temperature for $n\text{Bu}_4\text{NPF}_6$ (a) and $[\{\text{Cu}(\text{dppe})\}_3\{\text{hat}(\text{CN})_6\}](\text{PF}_6)_2$ (b) in CDCl_3 solution.

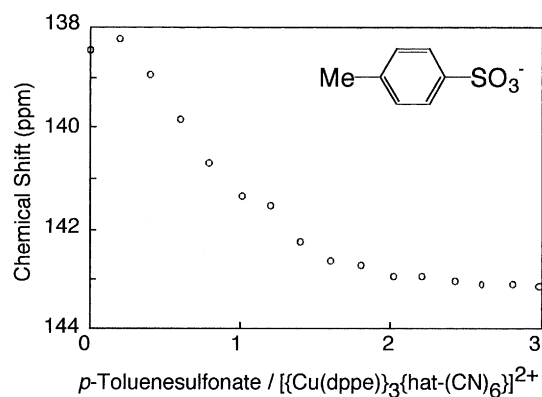


Fig. 28. Plot of ^{31}P -NMR chemical shifts against $[\text{p-toluenesulfonate}]/[\text{radical complex}]$.

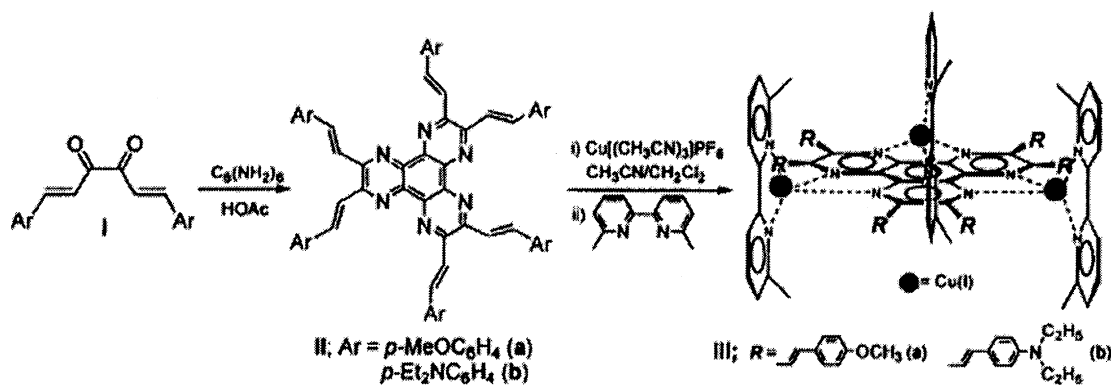


Fig. 29. Synthesis of the octupolar molecules based on hat derivatives (original Scheme 1 from Ref. [47]).

spectrum, however, exhibits a relatively more important contribution of the lowest energy band (500–590 nm) characteristic of Ru–hat complexes. Therefore, an energy transfer would take place from the Ru–hat ³MLCT state towards the Ir–hat ³SBLCT (mixed with ³MLCT character) in [$\{\text{Ru}(\text{bpy})_2\}\{\text{Ir}(\text{ppy})_2(\text{hat})\}^{3+}$].

There is an expanding interest in the interaction of transition metal complexes with nucleic acids, a major reason being the effectiveness of such complexes as chemotherapeutic agents [42]. In the presence of mononucleotides and different polynucleotides, the photophysical and photochemical properties of mononuclear and binuclear ruthenium(II) complexes, $[\text{Ru}(\text{bpy})(\text{hat})_2]^{2+}$ (1b type) and $[\{\text{Ru}(\text{phen})_2\}_2(\text{hat})]^{4+}$ (2a type), have been examined [43–45]. The monometallic complex undergoes visible light-induced electron transfer from guanine, forming a photoadduct. On the other hand, characteristics features, not observed with monometallic ruthenium(II) complexes, appear with this dimeric compound. First it forms strong ion pairs with mononucleotides adenosine- and guanosine-5'-monophosphate, detected from the absorption and emission characteristics under steady state and time-resolved conditions. Secondly, under steady state illumination, very weak luminescence enhancements are induced by the addition of double stranded calf thymus DNA (CT-DNA) whereas important increases of emission occur by the addition of denatured CT-DNA. This is understandable taking into account the dimensions of the dinuclear complex when compared to those of the double stranded DNA grooves.

4.3. Nonlinear optics

The metal complexes of hat and its derivatives are promising candidates for nonlinear optical materials because it is expected that charge transfer transitions from metal ions to the hat ligand with low lying π^* orbitals will enhance the optical nonlinearity. The third-order nonlinear optical properties have been reported for a copper(I) trinuclear complex $[\{\text{Cu}(\text{dppe})\}_3\{\text{hat}(\text{CN})_6\}](\text{PF}_6)_2$ [46]. The third-order NLO susceptibility $\chi^{(3)}(-\omega; \omega, 0, 0)$ can

be obtained from the electroabsorption spectra, i.e. electric field-induced absorption change measured on a spin-coated poly(methylmethacrylate) thin film doped with the complex. The $\chi^{(3)}(-\omega; \omega, 0, 0)$ value of this complex is 1.7×10^{-32} esu cm³, which is comparable to those of phthalocyanines, e.g. 2.7×10^{-32} and 1.1×10^{-32} esu cm³ for $\text{H}_2\text{Pc}(\text{tBu})_4$ and $\text{PbPc}(\text{tBu})_4$, respectively, indicating that the intramolecular charge transfer transition from copper(I) to hat-(CN)₆ enhances the third-order nonlinear susceptibility.

Octupolar molecules with C_3 symmetry exhibit a first hyperpolarizability comparable to those for the donor–acceptor dipoles [47]. Because the hat derivatives have not only a C_3 symmetrical structure but also an electron-accepting hexaaza core, the introduction of electron-donating substituents such as *p*-methoxy- and *p*-dialkylaminostyryl groups at the 2, 3, 6, 7, 10, 11-positions of hat would produce octupolar molecules (Fig. 29). Furthermore, the β values of these compounds can easily be optimised by changing the donor and acceptor strength, either by substituting a different electron-donating group at the *para* positions of the styryl moieties or by coordinating the hexaaze groups with metal ions. The linear and nonlinear optical properties of the four chromophores were measured and are summarised in Table 5. The λ_{max} values are shifted to a longer wavelength as the donor strength is increased. A similar red shift is observed as the acceptor is made more electron-deficient as a result of coordination to copper(I) ions, forming 3a-type complexes. For these compounds, the β values increase as the acceptor strength is increased by the coordination of the hat moiety to copper(I) ions at the center of the octupolar molecules. These results are consistent with the theoretical prediction that the β value should increase as the donor and acceptor strength is increased.

4.4. Magnetic properties

The design of coupled systems with strong magnetic interactions between distant metal centers is an emerging field for inorganic chemists. Variable-temperature magnetic susceptibility data have been measured [32] for the three paramagnetic one-dimensional chains, $[\{\text{Cu}_4(\text{hat})_2\text{Cl}_8\} \cdot 6\text{H}_2\text{O}]_n$

Table 5
Optical properties of hat derivatives and their Cu(I) complexes

Compound	$\lambda_{\text{max}}/\text{nm}$ ($\log \epsilon$)	β , 10^{-30} esu	$\beta(0)$, 10^{-30} esu
hat-(C=CPhOMe) ₆	460(4.49)	18	11
hat-(C=CPhN(Et) ₂) ₆	526(4.90)	50	29
[{Cu(Me ₂ bpy)} ₃ {hat-(C=CPhOMe) ₆ }] (PF ₆) ₂	468(4.90)	31	18
[{Cu(Me ₂ bpy)} ₃ {hat-(C=CPhN(Et) ₂) ₆ }] (PF ₆) ₂	532(4.55)	197	93

(2d type), {[Cu(hat)(H₂O)₂](NO₃)₂]_n (2c type), and {[Cu₂(hat)(H₂O)₆](SO₄)₂·2H₂O]_n (3b type) (Figs. 19–21). For the bis-bidentate chains, {[Cu₄(hat)₂Cl₈]·6H₂O]_n and {[Cu(hat)(H₂O)₂](NO₃)₂]_n, the magnetic susceptibility data reveal the occurrence of weak intramolecular antiferromagnetic interactions between copper(II) ions through the bridging hat, the *J* values being -2.5 ([Cu₄(hat)₂Cl₈]·6H₂O]_n) and -2.1 cm^{-1} ([Cu(hat)(H₂O)₂](NO₃)₂]_n). In {[Cu₄(hat)₂Cl₈]·6H₂O]_n the interaction across the di- μ -chloro bridge within the tetranuclear entity is found to be weak and ferromagnetic in character (ca. $+0.7 \text{ cm}^{-1}$). As far as the treatment of the magnetic data of 3b-type complex {[Cu₂(hat)(H₂O)₆](SO₄)₂·2H₂O]_n is concerned, one can see that the structure of this complex is made up of chains of hat-bridged triangles of copper(II) ions (Fig. 21). No theoretical model has been developed for the spin topology that will result from a chain of triangles in which the magnetic interaction through all three edges is operative. However, the magnetic behaviour of {[Cu₂(hat)(H₂O)₆](SO₄)₂·2H₂O]_n was analysed through the expression for a uniformly spaced copper(II) chain plus an isolated spin doublet, indicating the occurrence of a weak intramolecular antiferromagnetic interaction between the copper(II) ions constructing the coordination chain, the *J* value being -2.4 cm^{-1} .

Three paramagnetic cobalt(II)-assembled complexes, [Co₆{hat-(COO)₆}]²⁴⁻ (Fig. 11) [24], [Co₄(hat)₄Cl₈] (Fig. 12) [25], and {[Co₃(hat){N(CN)₂}(H₂O)₂}]_n (3c type in Fig. 3) [33], have been isolated to date. Although the crystal structures of these complexes are fascinating, magnetic exchange through the hat ligand, is however, negligible compared to the zero-field splitting of the cobalt(II) centers.

5. Conclusion

During the last decade, considerable effort has been devoted to the synthesis of metal complexes with hat and its derivatives, because they possess not only three chelating sites to construct supramolecular metal-assembled systems but also large electron-deficient π -systems. From the spatial structural point of view, various types of metal complexes have been synthesized, whose motif range from mononuclear, oligonuclear to infinite forms. However, these compounds usually result in aesthetics, still apart from the world of functionalism. On the other hand, the physicochemical properties have been studied for the last decade, focusing on mono-, bi-, trinuclear complexes as well as metal-free

compounds. Fortunately, several compounds based on hat cores have been created, which possess functionality such as nonlinear optics, anion trapping, molecular receptor, DNA photoprobe, magnetism and other physicochemical properties, successfully reflecting potential advantages of hat derivatives. Application of this functionality into polynuclear and/or infinite metal-assembled complexes is of particular interest but still embryonic. Further improvement of these compounds is required in these areas: (1) microporous properties; (2) magnetism; (3) nonlinear optics; and (4) conductivities. The new functional chemistry for polynuclear complexes with hat and its derivatives has just begun and will provide us with fruitful compound-based materials.

Acknowledgements

This work was partially supported by the Japan Society for the Promotion of Science, and Grants for Scientific Research from the Ministry of Education, Science, and Culture, Japan.

References

- [1] D.Z. Rogers, J. Org. Chem. 51 (1986) 3904.
- [2] R. Nasielski-Hinkens, M. Benedek-Vamos, D. Maetens, J. Nasielski, J. Organometallic Chem. 217 (1981) 179.
- [3] B. Kohne, K. Praefcke, Liebigs Ann. Chem. (1985) 522.
- [4] J.T. Rademacher, K. Kanakarajan, A.W. Czarnik, Synthesis (1994) 378.
- [5] K. Kanakarajan, A.W. Czarnik, J. Org. Chem. 51 (1986) 5241.
- [6] K. Kanakarajan, A.W. Czarnik, Polymer Commun. 30 (1989) 171.
- [7] M.S.P. Sarma, A.W. Czarnik, Synthesis (1988) 72.
- [8] A. Masschelein, A. Kirsch-De Mesmaeker, C. Verhoeven, R. Nasielski-Hinkens, Inorg. Chim. Acta 129 (1987) L13.
- [9] A. Kirsch-De Mesmaeker, L. Jacquet, A. Masschelein, F. Vanhecke, K. Heremans, Inorg. Chem. 28 (1989) 2465.
- [10] I. Ortmans, P. Didier, A. Kirsch-De Mesmaeker, Inorg. Chem. 34 (1995) 3695.
- [11] L. Jacquet, A. Kirsch-De Mesmaeker, J. Chem. Soc. Faraday Trans. 88 (1992) 2471.
- [12] L. Tan-Sien-Hee, A. Kirsch-De Mesmaeker, J. Chem. Soc. Dalton Trans. (1994) 3651.
- [13] P. Didier, L. Jacquet, A. Kirsch-De Mesmaeker, R. Hueber, A. Van Dorsseleer, Inorg. Chem. 31 (1992) 4803.
- [14] R. Sahai, P. Rillema, R. Shaver, S. Van Wallendael, D.C. Jackman, M. Boldaji, Inorg. Chem. 28 (1989) 1022.
- [15] T.J. Rutherford, O.V. Gijte, A. Kirsch-De Mesmaeker, F.R. Keene, Inorg. Chem. 36 (1997) 4465.
- [16] T.J. Rutherford, F.R. Keene, Inorg. Chem. 36 (1997) 3580.
- [17] T. Okubo, S. Kitagawa, M. Kondo, H. Matsuzaka, T. Ishii, Angew. Chem. Int. Ed. 38 (1999) 931.

- [18] J.-M. Lehn, *Supramolecular Chemistry: Concepts and Perspectives* (1995) VCH.
- [19] P. Baxter, J.-M. Lehn, A. DeCian, J. Fischer, *Angew. Chem. Int. Ed.* 32 (1993) 69.
- [20] A. Marquis-Rigault, A. Dupont-Gervais, P.N.W. Baxter, A.V. Dorselaer, J.-M. Lehn, *Inorg. Chem.* 35 (1996) 2307.
- [21] P.N.W. Baxter, J.-M. Lehn, B.O. Knersel, G. Baum, D. Feske, *Chem. Eur. J.* 5 (1999) 113.
- [22] M. Fujita, J. Yazaki, K. Ogura, *J. Am. Chem. Soc.* 112 (1990) 5645.
- [23] S. Leininger, B. Olenyuk, P.J. Stang, *Chem. Rev.* 100 (2000) 853.
- [24] S. Masaoka, S. Furukawa, H.-C. Chang, T. Mizutani, S. Kitagawa, *Angew. Chem. Int. Ed.* 40 (2001) 3817.
- [25] J.R. Galán-Mascarós, K.R. Dunbar, *Chem. Commun.* (2001) 217.
- [26] G.R. Newkome, C.N. Moorefield, F. Vögtle, *Dendritic Molecules* (1996) Verlag Chemie.
- [27] C. Moucheron, A. Kirsch-De Mesmaeker, *J. Am. Chem. Soc.* 118 (1996) 12834.
- [28] L. Latterini, G. Pourtois, C. Moucheron, R. Lazzaroni, J.-L. Brédas, A. Kirsch-De Mesmaeker, F.C. De Schryver, *Chem. Eur. J.* 6 (2000) 1331.
- [29] J.C. Beeson, L.J. Fitzgerald, J.C. Gallucci, R.E. Gerkin, J.T. Rademacher, A.W. Czarnik, *J. Am. Chem. Soc.* 116 (1994) 4621.
- [30] H. Grove, J. Sletten, M. Julve, F. Lloret, L. Lezama, J. Carranza, S. Parsons, P. Rillema, *J. Mol. Struct.* 606 (2002) 253.
- [31] V.J. Catalano, W.E. Larson, M.M. Olmstead, H.B. Gray, *Inorg. Chem.* 33 (1994) 4502.
- [32] H. Grove, J. Sletten, M. Julve, F. Lloret, *J. Chem. Soc. Dalton Trans.* (2001) 1029.
- [33] S.R. Marshall, A.L. Rheingold, L.N. Dawe, W.W. Shum, C. Kitamura, J.S. Miller, *Inorg. Chem.* 41 (2002) 3599.
- [34] B.F. Abrahams, P.A. Jackson, R. Robson, *Angew. Chem. Int. Ed.* 37 (1998) 2656.
- [35] I.Y. Bagryanskaya, Y.V. Gatilov, *Zh. Strukt. Khim.* 24 (1983) 158.
- [36] X.-H. Bu, K. Biradha, T. Yamaguchi, M. Nishimura, T. Ito, K. Tanaka, M. Shionoya, *Chem. Commun.* (2000) 1953.
- [37] A. Bianchi, K. Bowman-James, A. Garcia-Espana, *Supramolecular Chemistry of Anions* (1997) VHC.
- [38] A. Juris, V. Balzani, F. Barigelletti, S. Campagna, P. Belser, A. von Zelewsky, *Coord. Chem. Rev.* 84 (1988) 85.
- [39] K. Kalyanasundaram, *Coord. Chem. Rev.* 46 (1982) 159.
- [40] F.R. Keene, *Chem. Soc. Rev.* 27 (1998) 185.
- [41] B.D. Yeomans, L.S. Kelso, P.A. Tregloan, F.R. Keene, *Eur. J. Inorg. Chem.* (2001) 239.
- [42] A. Siegel, H. Siegel, *Metal Ions in Biological Systems*, Vols. 32 and 33, Marcel Dekker, New York, 1996.
- [43] O.V. Gijte, A.K.-D. Mesmaeker, *J. Chem. Soc. Dalton Trans.* (1999) 951.
- [44] J.-P. Lecomte, A.K.-D. Mesmaeker, M.M. Feeney, J.M. Kelly, *Inorg. Chem.* 34 (1995) 6481.
- [45] L. Jacquet, R. Jeremy, H. Davies, A.K.-D. Mesmaeker, J.M. Kelly, *J. Am. Chem. Soc.* 119 (1997) 11763.
- [46] T. Okubo, S. Kitagawa, S. Masaoka, S. Furukawa, M. Kondo, T. Noh, T. Isoshima, T. Wada, H. Sasabe, *Nonlinear Optics* 24 (2000) 129.
- [47] B.R. Cho, S.K. Lee, K.A. Kim, K.N. Son, T.I. Kang, S.J. Jeon, *Tetrahedron Lett.* 39 (1998) 9205.